

An augmented space approach to the study of random ternary alloys: II. Optical response

This article has been downloaded from IOPscience. Please scroll down to see the full text article.

2009 J. Phys.: Condens. Matter 21 195504

(<http://iopscience.iop.org/0953-8984/21/19/195504>)

View [the table of contents for this issue](#), or go to the [journal homepage](#) for more

Download details:

IP Address: 129.252.86.83

The article was downloaded on 29/05/2010 at 19:34

Please note that [terms and conditions apply](#).

An augmented space approach to the study of random ternary alloys: II. Optical response

Kartick Tarafder¹ and Abhijit Mookerjee²

¹ Division of Materials Theory, Department of Physics and Materials Science, Uppsala University, Box 530, 751 21 Uppsala, Sweden

² Advanced Materials Research Unit, S N Bose National Center for Basic Sciences, JD Block, Sector III, Salt Lake City, Kolkata 700 098, India

Received 31 October 2008, in final form 31 March 2009

Published 22 April 2009

Online at stacks.iop.org/JPhysCM/21/195504

Abstract

The augmented space approach to the study of random ternary alloys, described in an earlier paper (Alam and Mookerjee 2009 *J. Phys.: Condens. Matter* **21** 195503), has been combined with the generalized recursion method of Viswanath and Müller (1993 *The User Friendly Recursion Method*, (Troisième Cycle de la Physique, en Suisse Romande)) and the tight-binding linear muffin-tin orbitals technique (TB-LMTO) to study the optical response in disordered $\text{Cu}_x\text{Ni}_y\text{Zn}_z$ alloys, and compared with existing experimental results.

(Some figures in this article are in colour only in the electronic version)

1. Introduction

First principles electronic structure calculations of multi-component disordered alloys has been a challenging problem. The absence of lattice translational symmetry is the main obstacle to the construction of a quantitative theory, comparable in accuracy and efficiency with those for ordered crystalline solids. The situation becomes more difficult when the types of constituent atoms are more than two. The majority of electronic structure calculations for disordered alloys have dealt with binary substitutional alloys, whereas most alloys of practical interest are multi-component. Binary alloy systems provide us with a first step in the understanding of higher-order alloy systems. In addition, many systems, like binary alloys with vacancies or binary magnetic alloys with random moments, can also be thought of as special cases of more general higher-order alloys. The study of optical properties for these multi-component alloys systems is an important tool in understanding and characterizing them. In this paper we shall proceed from our earlier work [1] on the augmented space recursion (ASR) technique for calculating the electronic structure for ternary alloys, and combine this with the generalized recursion method of Viswanath and Müller [2] to study the optical properties for ternary alloys.

In section 2 we shall first generalize the augmented space formalism for optical properties for ternary alloys. In section 4

we shall apply our methodology to $\text{Cu}_x\text{Ni}_y\text{Zn}_z$ alloys. The motivation behind the choice of this alloy is that there are experimental data available in the literature which will help us to confirm the validity and accuracy of our proposed methodology.

2. Configuration averaging using augmented space approach

The ideas behind the augmented space approach to the study of the electronic structure of random ternary alloys have been described in great detail in an earlier communication [1]. Here we shall briefly introduce only those essential points which will enable us to apply the methodology to study the optical response in random ternary alloys.

- (i) The first thing to note is that any set of uncorrelated random local potential parameters in the ternary alloys can be written in terms of ternary random variables $\{n_R\}$, where each n_R takes values 1, 0, -1 , corresponding to whether the site R is occupied by A, B or C type of atoms, with probabilities proportional to their concentrations: x, y, z where $x + y + z = 1$.
- (ii) The augmented space approach [3] expresses the probability densities $p(n_R) = x\delta(n_R - 1) + y\delta(n_R) + z\delta(n_R + 1)$ as the projected spectral densities of operators

$\{N_R\}$, whose eigenvalues are 1, 0 and -1 , the values taken by n_R , and the corresponding eigenstates $|1\rangle$, $|0\rangle$ and $|\bar{1}\rangle$ are its ‘configuration’ states:

$$p(n_R) = -\frac{1}{\pi} \lim_{\delta \rightarrow 0} \text{Im}\langle \emptyset | ((n + i\delta)I - N_R)^{-1} | \emptyset \rangle. \quad (1)$$

The projection is on to the ‘average’ state $|\emptyset\rangle = \sqrt{x}|1\rangle + \sqrt{y}|0\rangle + \sqrt{z}|\bar{1}\rangle$.

- (iii) We work in a new basis of representation: $|0\rangle = |\emptyset\rangle$, $|\{1\}\rangle$ and $|\{2\}\rangle$: which is the ‘average’ state and two other linear combinations of the ‘configuration’ states which are all mutually orthogonal. These three states span the configuration space ϕ_R of n_R (of rank 3).
- (iv) In this basis the representations of N_R and $M_R = N_R^2$ are:

$$N_R = \begin{pmatrix} \alpha_1 & \beta_1 & 0 \\ \beta_1 & \alpha_2 & \beta_2 \\ 0 & \beta_2 & \alpha_3 \end{pmatrix}$$

$$M_R = \begin{pmatrix} A_1 & B_{12} & B_{13} \\ B_{12} & A_2 & B_{23} \\ B_{13} & B_{23} & A_3 \end{pmatrix}$$

where,

$$\alpha_1 = (x_A - x_C)$$

$$\alpha_2 = N_1^2 [(x_A - x_C)(x_B^2 - 4x_A x_C)]$$

$$\alpha_3 = \frac{x_B(x_A - x_C)}{-x_A - x_C + (x_A - x_C)^2} \quad \beta_1^2 = \frac{1}{N_1^2}$$

$$\frac{1}{N_1^2} = (x_A + x_C) - (x_A - x_C)^2$$

$$\beta_2^2 = x_B + \frac{x_B(x_A - x_C)}{(x_A + x_C) - (x_A - x_C)^2}$$

$$\times \left[(x_A - x_C) - \frac{x_B(x_A - x_C)}{(x_A + x_C) - (x_A - x_C)^2} \right]$$

$$A_1 = \alpha_1^2 + \beta_1^2, \quad A_2 = \alpha_2^2 + \beta_1^2 + \beta_2^2$$

$$A_3 = \alpha_3^2 + \beta_2^2 \quad B_{12} = (\alpha_1 + \alpha_2)\beta_1$$

$$B_{13} = \beta_1\beta_2 \quad B_{23} = (\alpha_3 + \alpha_2)\beta_2.$$

- (v) The operators in full configuration space $\Phi = \prod_R^\otimes \phi_R$ are:

$$\tilde{N}_R = \alpha_1 \tilde{\mathcal{P}}_R^0 + \alpha_2 \tilde{\mathcal{P}}_R^1 + \alpha_3 \tilde{\mathcal{P}}_R^2 + \beta_1 \tilde{\mathcal{T}}_R^{01} + \beta_2 \tilde{\mathcal{T}}_R^{12}$$

$$\tilde{M}_R = A_1 \tilde{\mathcal{P}}_R^0 + A_2 \tilde{\mathcal{P}}_R^1 + A_3 \tilde{\mathcal{P}}_R^2 + B_{12} \tilde{\mathcal{T}}_R^{01} + B_{23} \tilde{\mathcal{T}}_R^{12} + B_{13} \tilde{\mathcal{T}}_R^{02}, \quad (2)$$

here, $\tilde{\mathcal{P}}_R^\lambda = I \otimes I \otimes \dots \otimes |\lambda_R\rangle\langle\lambda_R| \otimes \dots$ and $\tilde{\mathcal{T}}_R^{\lambda\lambda'} = I \otimes I \otimes \dots \otimes (|\lambda_R\rangle\langle\lambda'_R| + |\lambda'_R\rangle\langle\lambda_R|) \otimes \dots$ where $\lambda = 0, 1, 2$. The projection operator counts the number of configuration fluctuations at the site R , while the transfer operators create or annihilate configuration fluctuations at the site R .

- (vi) Any random local potential parameter X_R in the Hamiltonian now can be expressed in terms of n_R as:

$$X_R = \frac{1}{2} n_R(1 + n_R) X_A + (1 - n_R)(1 + n_R) X_B + \frac{1}{2} n_R(n_R - 1) X_C$$

where X_A, X_B, X_C are the values taken by X_R , corresponding to the random variable n_R having the values

1, 0, -1 , respectively. The augmented space theorem replaces n_R by the corresponding operator N_R , and n_R^2 by $M_R = N_R^2$, X_R is replaced by an operator \tilde{X}_R in the ‘configuration’ space spanned by the ‘configuration’ states of N_R , and can be written as:

$$\tilde{X}_R = X_B \tilde{I} + \frac{1}{2}(X^A - X^C) \tilde{N}_R + \frac{1}{2}(X_A - 2X_B + X_C) \tilde{M}_R. \quad (3)$$

- (vii) For the realistic calculations we start from the TB-LMTO Hamiltonian. The equation (3) then gives us a prescription of how to set up the augmented space operators corresponding to the potential parameters C_{RL}, Δ_{RL} and o_{RL} . The second order TB-LMTO Hamiltonian has the familiar form:

$$\tilde{H} = \tilde{E}_L^v + \tilde{h} - \tilde{h} \tilde{o} \tilde{h}$$

$$\tilde{h} = \sum_{RL} (\tilde{C}_{RL} - E_L^v) \otimes \mathcal{P}_{RL} + \sum_{RL, R'L'} \tilde{\Delta}_{RL}^{1/2} \tilde{\mathcal{S}}_{RL, R'L'} \tilde{\Delta}_{R'L'}^{1/2} \otimes \mathcal{T}_{RL, R'L'}, \quad (4)$$

where L is the composite index of $(\alpha l m \sigma)$. \mathcal{P}_{RL} , and $\mathcal{T}_{RL, R'L'}$ are projection and transfer operators in the Hilbert space \mathcal{H} spanned by the basis $\{|RL\rangle\}$, respectively. $\tilde{C}_{RL}, \tilde{\Delta}_{RL}^{1/2}$ and \tilde{o}_{RL} are operators in the configuration space of n_R and have the same form as \tilde{X}_R described above. The Hamiltonian is a function of a whole set of random variables $\{n_R\}$, one for each site. The configuration space of the whole set is $\Phi = \prod^\otimes \phi_R$, where ϕ_R is the configuration space of the variable n_R and is spanned by the three eigenstates of N_R . The augmented Hamiltonian \tilde{H} is an operator in the augmented space $\Psi = \mathcal{H} \otimes \Phi$.

- (viii) The augmented space theorem [3] tells us that the configuration average of any function of $\{n_R\}$ is:

$$\langle\langle f[H(\{n_R\})] \rangle\rangle = \langle\langle \emptyset | f[\tilde{H}(\{\tilde{N}_R, \tilde{M}_R\})] | \emptyset \rangle\rangle \quad (5)$$

where $|\langle\emptyset\rangle\rangle = |\prod_R^\otimes \langle 0_R \rangle\rangle$.

3. Optical response in disordered ternary alloys

3.1. The generalized recursion

In this section we shall discuss a new method for the calculation of optical conductivity of disordered ternary alloys. The idea of this generalized recursion method was proposed by Viswanath and Müller [2]. It is based on the linear response theory. If we consider an electro-magnetic field as the perturbing field, the equation for the linear current response in the system is:

$$\langle\langle \mathcal{J}^\mu(t) \rangle\rangle = \int_{-\infty}^{\infty} \chi^{\mu\nu}(t-t') A^\nu(t') \quad (6)$$

where, $A^\nu(t)$ is the vector potential, and the response function (which is the generalized susceptibility) can be written as:

$$\chi^{\mu\nu}(t-t') = (i/\hbar) \Theta(t-t') \langle\langle [\mathcal{J}^\mu(t), \mathcal{J}^\nu(t')] \rangle\rangle, \quad (7)$$

where \mathbf{j}^μ is the current operator and Θ is the Heaviside step function. If the underlying lattice has cubic symmetry, $\chi^{\mu\nu} = \chi \delta_{\mu\nu}$. The fluctuation dissipation theorem then relates the imaginary part of the Laplace transform of the response function, i.e. the generalized susceptibility, to the Laplace transform of a correlation function:

$$\chi''(\omega) = (1/2\hbar) (1 - \exp\{-\beta\hbar\omega\}) S(\omega) \quad (8)$$

where,

$$S(\omega) = \int_0^\infty dt \exp\{i(\omega + i\delta)t\} \text{Tr}(\mathcal{J}^\mu(t) \mathcal{J}^\mu(0)). \quad (9)$$

Since the response function is independent of the direction label μ for cubic symmetry, in the following we shall drop this symbol. In case of other symmetries we can generalize our results for different directions. From the above discussion, it is clear that for given a quantum ‘Hamiltonian’ H , our goal is to obtain the correlation function,

$$S(t) = \frac{1}{N} \sum_R \langle R | \mathcal{J}(t) \mathcal{J}(0) | R \rangle = \langle R | \mathcal{J}(t) \mathcal{J}(0) | R \rangle. \quad (10)$$

This will be true if translational symmetry holds and the last expression is independent of the label R . The correlation function can be determined directly via the recursion method, as described in our earlier paper [4]. In order to simplify the expressions for the dynamical quantities as produced by the Hamiltonian, we consider henceforth the modified Hamiltonian $\tilde{H} = H - E_0 I$, whose band energy is shifted to zero. Let

$$|\psi(t)\rangle = \mathcal{J}(t) |\phi\rangle. \quad (11)$$

The time evolution of this *ket* is governed by the Schrödinger equation

$$-i \frac{d}{dt} \{|\psi(t)\rangle\} = \tilde{H} |\psi(t)\rangle. \quad (12)$$

We shall now generate an orthogonal basis $\{|f_k\rangle\}$ for representation of equation (12). which can be done in the following way.

(i) We begin with initial conditions:

$$|f_{-1}\rangle = 0; \quad |f_0\rangle = \mathcal{J}(0) |R\rangle.$$

(ii) We now generate the new basis members by a three term recurrence relationship:

$$|f_{k+1}\rangle = \tilde{H} |f_k\rangle - \alpha_k |f_k\rangle - \beta_k^2 |f_{k-1}\rangle \quad k = 0, 1, 2 \dots$$

where,

$$\alpha_k = \frac{\langle f_k | \tilde{H} | f_k \rangle}{\langle f_k | f_k \rangle} \quad \beta_k^2 = \frac{\langle f_k | f_k \rangle}{\langle f_{k-1} | f_{k-1} \rangle}. \quad (13)$$

We now expand the bra $\langle \psi(t) |$ in this orthogonal basis:

$$\langle \psi(t) | = \sum_{k=0}^{\infty} D_k(t) \langle f_k |. \quad (14)$$

Substituting equation (14) into equation (12) and using the orthogonality of the basis, we get:

$$-i \dot{D}_k(t) = D_{k-1}(t) + \alpha_k D_k(t) + \beta_{k+1}^2 D_{k+1}(t) \quad (15)$$

with $D_{-1}(t) = 0$ and $D_k(0) = \delta_{k,0}$. We shall now show that the pair of sequences generated by us, namely, $\{\alpha_k\}$ and $\{\beta_k^2\}$, are enough to generate the correlation function. We first note that:

$$D_0(t) = \langle f_0 | \psi(t) \rangle = S(t). \quad (16)$$

If $d_k(z)$ is the Laplace transform of $D_k(t)$, it also satisfies a three term recurrence:

$$(z - \alpha_k) d_k(z) - i \delta_{k,0} = d_{k-1}(z) + \beta_{k+1}^2 d_{k+1}(z) \quad k = 0, 1, 2 \dots \quad (17)$$

This set of equations can be solved for $d_0(z)$ as a continued fraction representation:

$$d_0(z) = \frac{i}{z - \alpha_0 - \frac{\beta_1^2}{z - \alpha_1 - \frac{\beta_2^2}{z - \alpha_2 - \dots}}}. \quad (18)$$

The structure function, which is the Laplace transform of the correlation function, can then be obtained from the above:

$$S(\omega) = \lim_{\delta \rightarrow 0} 2 \text{Re} d_0(\omega + i\delta). \quad (19)$$

In case of a disordered alloy, we notice that $S(t) = S[\tilde{H}(\{n_R\})]$ is a function of the random variable n_R and we need to calculate the configuration averaged value. Therefore we use the augmented space formalism and, applying the augmented space theorem [3], we can write:

$$\langle \langle S(t) \rangle \rangle = \langle R \otimes \{\emptyset\} | \tilde{\mathcal{J}}(t) \tilde{\mathcal{J}}(0) | R \otimes \{\emptyset\} \rangle = S[\tilde{H}(\{\tilde{N}_R, \tilde{M}_R\})] \quad (20)$$

where the augmented space Hamiltonian \tilde{H} and the current operators $\tilde{\mathcal{J}}(t)$ are constructed by replacing every random variable n_R and n_R^2 by the corresponding operators \tilde{N}_R and \tilde{M}_R . The recursion may now be modified step by step in the full augmented space:

$$\tilde{D}_0(t) = \langle f_0 | \{\emptyset\} \otimes \psi(t) \rangle = \langle \langle S(t) \rangle \rangle \quad (21)$$

where $|f_0\rangle = \tilde{\mathcal{J}}(0) |R \otimes \{\emptyset\}\rangle$ and,

$$\tilde{d}_0(z) = \frac{i}{z - \tilde{\alpha}_0 - \frac{\tilde{\beta}_1^2}{z - \tilde{\alpha}_1 - \frac{\tilde{\beta}_2^2}{z - \tilde{\alpha}_2 - \dots}}}. \quad (22)$$

The configuration averaged structure function, which is the Laplace transform of the averaged correlation function, can then be obtained from the above:

$$\langle \langle S(\omega) \rangle \rangle = \lim_{\delta \rightarrow 0} 2 \text{Re} \tilde{d}_0(\omega + i\delta) \quad (23)$$

3.2. Construction of the Hamiltonian and current operators in augmented space

As we have already mentioned, before we carry out the recursion in augmented space for the calculation configuration averaged correlation function, we need to construct the Hamiltonian and the current operator in augmented space. We shall start with a second order Hamiltonian for a random ternary alloy represented in the minimal basis of a tight-binding linear muffin-tin orbitals method (TB-LMTO). The TB-LMTO basis starts from the minimal muffin-tin orbitals of a Kohn–Korringa–Rostocker (KKR) formalism and then linearizes it by expanding around ‘nodal’ energy points $E_{v\ell}$. The wavefunction is then expressed as a linear combination of these basis functions:

$$\Phi_{jk}(\mathbf{r}) = \sum_{RL} c_{RL}^{jk} \left[\phi_{RL}(\mathbf{r}, E_{v\ell}) + \sum_{R'L'} h_{RLR'L'} \dot{\phi}_{R'L'}(\mathbf{r}, E_{v\ell}) \right],$$

where L is the composite index ($\alpha\ell m\sigma$), α labels the particular atom in the unit cell, $\ell m\sigma$ are the angular momenta-spin indices, j is the band index and R labels the unit cell. Here,

$$\phi_{RL}(\mathbf{r}, E_{v\ell}) = i^\ell Y_{\ell m}(\hat{r}) \phi_{R\ell}(r, E_{v\ell});$$

$$\dot{\phi}_{RL}(\mathbf{r}, E_{v\ell}) = i^\ell Y_{\ell m}(\hat{r}) \left. \frac{\partial \phi_{R\ell}(r, E)}{\partial E} \right|_{E=E_{v\ell}}.$$

The TB-LMTO secular equation provides the expansion coefficients c_{RL}^{jk} .

In this basis, the matrix elements of the current operator can be written as

$$\begin{aligned} J_{RL,R'L'}^\mu &= \left[V_{RL,R'L'}^{(1),\mu} \delta_{RR'} \right. \\ &+ \sum_{L''} \left\{ V_{RL,R'L''}^{(2),\mu} h_{R'L'',R'L'} + h_{RL,R'L''} V_{R'L'',R'L'}^{(3),\mu} \right\} + \dots \\ &+ \sum_{R''L''} \sum_{L'''} h_{RL,R''L''} V_{R''L'',R'L''}^{(4),\mu} h_{R''L'',R'L'} \left. \right], \end{aligned} \quad (24)$$

where

$$V_{RL,R'L'}^{(1),\mu} = \int_{r < s_R} d^3\mathbf{r} \phi_{R'L'}^*(\mathbf{r}, E_{v\ell}) (-i\nabla^\mu) \phi_{RL}(\mathbf{r}, E_{v\ell})$$

$$V_{RL,R'L'}^{(2),\mu} = \int_{r < s_R} d^3\mathbf{r} \dot{\phi}_{R'L'}^*(\mathbf{r}, E_{v\ell}) (-i\nabla^\mu) \phi_{RL}(\mathbf{r}, E_{v\ell})$$

$$V_{RL,R'L'}^{(3),\mu} = \int_{r < s_R} d^3\mathbf{r} \phi_{R'L'}^*(\mathbf{r}, E_{v\ell}) (-i\nabla^\mu) \dot{\phi}_{RL}(\mathbf{r}, E_{v\ell})$$

$$V_{RL,R'L'}^{(4),\mu} = \int_{r < s_R} d^3\mathbf{r} \dot{\phi}_{R'L'}^*(\mathbf{r}, E_{v\ell}) (-i\nabla^\mu) \dot{\phi}_{RL}(\mathbf{r}, E_{v\ell}).$$

We shall use the prescription from Hobbs [5] to obtain the above matrix elements.

If we define the vector $\vec{\Gamma}_{LL'}$ to be a combination of Gaunt coefficients:

$$\begin{aligned} \vec{\Gamma}_{LL'} &= \sqrt{\frac{2\pi}{3}} \left[\left(G_{\ell',1,\ell}^{m',-1,m} - G_{\ell',1,\ell}^{m',1,m} \right) \hat{\mathbf{x}} \right. \\ &+ i \left(G_{\ell',1,\ell}^{m',-1,m} + G_{\ell',1,\ell}^{m',1,m} \right) \hat{\mathbf{y}} + \sqrt{2} G_{\ell',1,\ell}^{m',0,m} \hat{\mathbf{z}} \left. \right] \end{aligned}$$

and the following integrals:

$$\begin{aligned} \int_0^{s_R} \phi_{R\ell'}^*(r, E_{v\ell'}) \phi_{R\ell}(r, E_{v\ell}) r^3 dr &= I_R^{\ell\ell'}; \\ \int_0^{s_R} \phi_{R\ell'}^*(r, E_{v\ell'}) \dot{\phi}_{R\ell}(r, E_{v\ell}) r^3 dr &= J_R^{\ell\ell'} \\ \int_0^{s_R} \dot{\phi}_{R\ell'}^*(r, E_{v\ell'}) \phi_{R\ell}(r, E_{v\ell}) r^3 dr &= K_R^{\ell\ell'}. \end{aligned}$$

We now introduce the notation $(1/2)s_R^2(D_R^{v\ell} - D_R^{v\ell'} - 1) = \mathcal{D}_R^{\ell\ell'}$, where $D_R^{v\ell}$ are the logarithmic derivatives of $\phi_{R\ell}(r, E_{v\ell})$ at $r = s_R$, where s_R is the atomic sphere radius. These are obtained as parameters in the TB-LMTO routines.

Then the components of the matrix elements involved in the current operator become

$$\begin{aligned} V_{RL,R'L'}^{(1),\mu} &= i^{\ell-\ell'-1} \Gamma_{LL'}^\mu \\ &\times \left[(E_{v\ell} - E_{v\ell'}) I_R^{\ell\ell'} - \mathcal{D}_R^{\ell\ell'} \xi_{R\ell} \xi_{R\ell'} \right] \\ V_{RL,R'L'}^{(2),\mu} &= i^{\ell-\ell'-1} \Gamma_{LL'}^\mu \\ &\times \left[(E_{v\ell} - E_{v\ell'}) J_R^{\ell\ell'} + I_R^{\ell\ell'} - \mathcal{D}_R^{\ell\ell'} \eta_{R\ell} \xi_{R\ell'} \right] \\ V_{RL,R'L'}^{(3),\mu} &= i^{\ell-\ell'-1} \Gamma_{LL'}^\mu \\ &\times \left[(E_{v\ell} - E_{v\ell'}) J_R^{\ell\ell'} - I_R^{\ell\ell'} - \mathcal{D}_R^{\ell\ell'} \xi_{R\ell} \eta_{R\ell'} \right] \\ V_{RL,R'L'}^{(4),\mu} &= i^{\ell-\ell'-1} \Gamma_{LL'}^\mu \left[(E_{v\ell} - E_{v\ell'}) K_R^{\ell\ell'} \right. \\ &+ \left. J_R^{\ell\ell'} - J_R^{\ell\ell'} - \mathcal{D}_R^{\ell\ell'} \eta_{R\ell} \eta_{R\ell'} \right], \end{aligned} \quad (25)$$

here $\xi_{R\ell} = \phi_{R\ell}(s_R, E_{v\ell})$ and $\eta_{R\ell} = \dot{\phi}_{R\ell}(s_R, E_{v\ell})$.

Ideally the next step should be to calculate pair-wise currents, where the two end sites are occupied by atom pairs AA, BB, CC, AB, BC or AC embedded in the disordered medium. However a simpler first step would be to obtain these current terms from the pure A, B and C and from the ordered alloys AB, BC and AC.

The current operator in the ternary disordered system, unlike the Hamiltonian parameters which were local, leads to off-diagonal disorder. Intrinsically the single-site coherent potential approximation is unable to deal with such problems. The strength of the augmented space method comes to the fore. The current can be written as

$$\vec{J} = \sum_{RL} \vec{J}_{RL,RL} \mathcal{P}_{RL} + \sum_{RL,R'L'} \vec{J}_{RL,R'L'} \mathcal{T}_{RL,R'L'}. \quad (26)$$

The diagonal term of the current operator can be written as

$$\begin{aligned} \vec{J}_{RL,RL} &= \frac{n_R(n_R + 1)}{2} \vec{J}_{RL,RL}^{\text{AA}} + (1 - n_R^2) \vec{J}_{RL,RL}^{\text{BB}} \\ &+ \frac{n_R(n_R - 1)}{2} \vec{J}_{RL,RL}^{\text{CC}} \end{aligned} \quad (27)$$

while the off-diagonal term may be written as

$$\begin{aligned} \vec{J}_{RL,R'L'} &= \frac{n_R n_{R'} (n_R + 1) (n_{R'} + 1)}{4} \vec{J}_{RL,R'L'}^{\text{AA}} \\ &+ (1 - n_R^2) (1 - n_{R'}^2) \vec{J}_{RL,R'L'}^{\text{BB}} \dots \\ &\dots + \frac{n_R n_{R'} (n_R - 1) (n_{R'} - 1)}{4} \vec{J}_{RL,R'L'}^{\text{CC}} \dots \end{aligned}$$

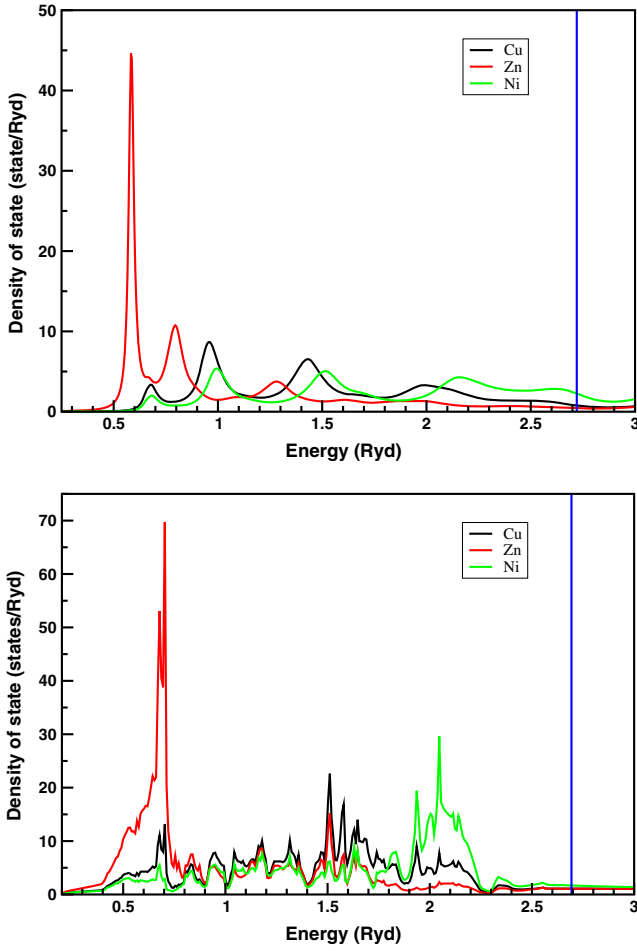


Figure 1. Atom projected density of states for $\text{Cu}_{50}\text{Zn}_{25}\text{Ni}_{25}$ ternary disordered (top) and ordered (bottom) alloy. The vertical (blue) line marks the Fermi energy.

$$\begin{aligned}
 & \dots + \left[\frac{n_R(n_R + 1)(1 - n_{R'}^2)}{2} \right. \\
 & \left. + \frac{n_{R'}(1 - n_R^2)(n_{R'} + 1)}{2} \right] \tilde{J}_{RL,R'L'}^{AB} \dots \\
 & \dots + \frac{n_R n_{R'}}{4} [(n_R + 1)(n_{R'} - 1) \\
 & + (n_R - 1)(n_{R'} + 1)] \tilde{J}_{RL,R'L'}^{AC} \dots \\
 & \dots + \left[\frac{(1 - n_R^2)(n_{R'} - 1)}{2} n_{R'} \right. \\
 & \left. + \frac{(n_R - 1)(1 - n_{R'}^2)}{2} n_R \right] \tilde{J}_{RL,R'L'}^{BC} \dots
 \end{aligned} \quad (28)$$

We need to express this current operator in augmented space. Replacing n_R by the corresponding operator \tilde{N}_R , and n_R^2 by \tilde{M}_R , we get

$$\tilde{J}_{RL,RL} = \tilde{J}_{RL,RL}^{BB} \tilde{I} + \tilde{J}_{RL,RL}^{(1)} \tilde{M}_R + \tilde{J}_{RL,RL}^{(2)} \tilde{N}_R \quad (29)$$

these operators either count or create/annihilate configuration fluctuations locally at sites R and

$$\begin{aligned}
 \tilde{J}_{RL,R'L'} &= \tilde{J}_{RL,R'L'}^{BB} \tilde{I} + \tilde{J}_{RL,R'L'}^{(3)} (\tilde{M}_R + \tilde{M}_{R'}) \\
 &+ \tilde{J}_{RL,R'L'}^{(4)} (\tilde{N}_R + \tilde{N}_{R'}) + \dots
 \end{aligned}$$

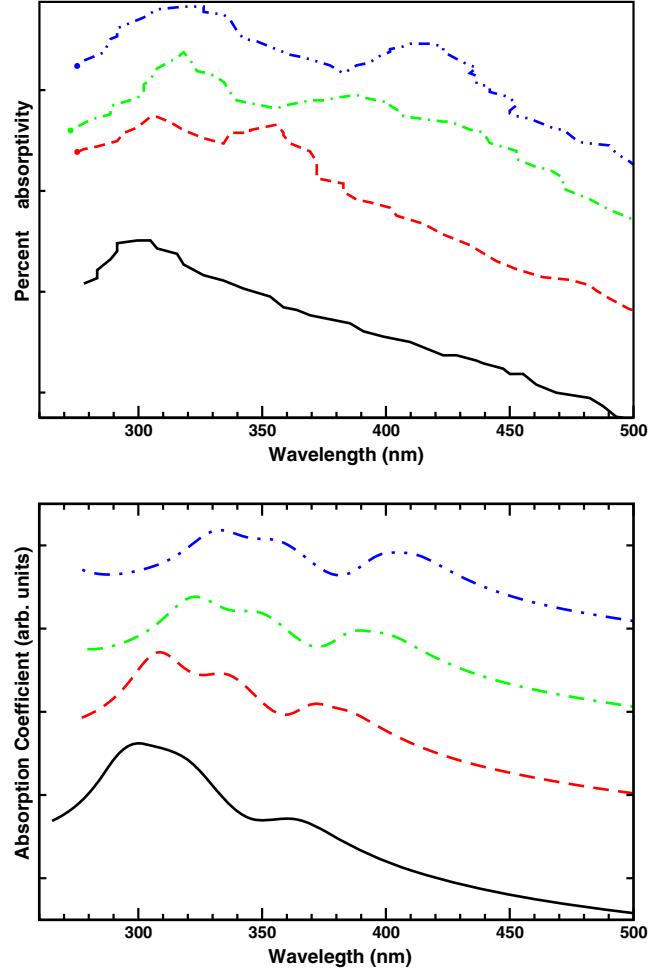


Figure 2. (Top) Experimentally observed absorptivity of $\text{Cu}_x\text{Ni}_y\text{Zn}_z$ disordered ternary alloy for four different compositions (from Schroder and Mamola [13]). (Bottom) Theoretical curve for the absorption coefficients of the same in the right side. The (black) full curves are for $\text{Cu}_{80}\text{Ni}_{10}\text{Zn}_{10}$, the (red) dashed curves are for $\text{Cu}_{76}\text{Ni}_9\text{Zn}_{15}$, the (green) dashed-dot curve is for $\text{Cu}_{70}\text{Ni}_9\text{Zn}_{21}$ and (blue) dashed-dot-dot curve is for $\text{Cu}_{66}\text{Ni}_8\text{Zn}_{26}$ alloy.

$$\begin{aligned}
 & \dots \tilde{J}_{RL,R'L'}^{(5)} \tilde{M}_R \otimes \tilde{M}_{R'} \\
 & + \tilde{J}_{RL,R'L'}^{(6)} (\tilde{M}_R \otimes \tilde{N}_{R'} + \tilde{N}_R \otimes \tilde{M}_{R'}) \\
 & + \tilde{J}_{RL,R'L'}^{(7)} \tilde{N}_R \otimes \tilde{N}_{R'}
 \end{aligned} \quad (30)$$

where

$$\begin{aligned}
 \tilde{J}_{RL,R'L'}^{(1)} &= \frac{1}{2} (\tilde{J}_{RL,R'L'}^{AA} + \tilde{J}_{RL,R'L'}^{CC} - 2\tilde{J}_{RL,R'L'}^{BB}) \\
 \tilde{J}_{RL,R'L'}^{(2)} &= \frac{1}{2} (\tilde{J}_{RL,R'L'}^{AA} - \tilde{J}_{RL,R'L'}^{CC}) \\
 \tilde{J}_{RL,R'L'}^{(3)} &= \frac{1}{2} (\tilde{J}_{RL,R'L'}^{AB} + \tilde{J}_{RL,R'L'}^{BC} - 2\tilde{J}_{RL,R'L'}^{BB}) \\
 \tilde{J}_{RL,R'L'}^{(4)} &= \frac{1}{2} (\tilde{J}_{RL,R'L'}^{AB} - \tilde{J}_{RL,R'L'}^{CB}) \\
 \tilde{J}_{RL,R'L'}^{(5)} &= \frac{1}{4} (\tilde{J}_{RL,R'L'}^{AA} + 4\tilde{J}_{RL,R'L'}^{BB} + \tilde{J}_{RL,R'L'}^{CC} \\
 & - 4\tilde{J}_{RL,R'L'}^{AB} + 2\tilde{J}_{RL,R'L'}^{AC} - 4\tilde{J}_{RL,R'L'}^{BC}) \\
 \tilde{J}_{RL,R'L'}^{(6)} &= \frac{1}{4} (\tilde{J}_{RL,R'L'}^{AA} - \tilde{J}_{RL,R'L'}^{CC} - 2\tilde{J}_{RL,R'L'}^{AB} + 2\tilde{J}_{RL,R'L'}^{BC}) \\
 \tilde{J}_{RL,R'L'}^{(7)} &= \frac{1}{4} (\tilde{J}_{RL,R'L'}^{AA} + \tilde{J}_{RL,R'L'}^{CC} - 2\tilde{J}_{RL,R'L'}^{AC}).
 \end{aligned} \quad (31)$$

It is easy to check that all the factors above vanish when the structure matrices are independent of site occupation (i.e. not random). The operators in the first line of equation (30) either count or create/annihilate configuration fluctuations at either of the two sites R and R' . The last four operators in the second line of equation (30) either count or create/annihilate configuration fluctuations *simultaneously* at both the sites R and R' . These operators are essentially *non-local* and cannot be dealt with in a local (single-site) mean-field approximation.

Once the Hamiltonian is set up, as in equation (4), and the current operators are set up, as in equations (29) and (30), we go back to our formulation of augmented space recursion, as described, and carry out the calculation for the configuration averaged optical response functions.

We use the augmented current operator to construct the starting state

$$|\psi(0)\rangle = \tilde{\mathcal{J}}^\mu |R \otimes \{\emptyset\}\rangle$$

and perform the recursion in augmented space to calculate the configuration averaged correlation function $\langle\langle S(\omega) \rangle\rangle$. Finally, the imaginary part of the dielectric function is related to this correlation function through:

$$\epsilon_2(\omega) = 4\pi \frac{\langle\langle S(\omega) \rangle\rangle}{\omega^2}. \quad (32)$$

The real part of the dielectric function $\epsilon_1(\omega)$ is related to the imaginary part $\epsilon_2(\omega)$ by a Kramer's Krönig relationship:

$$\epsilon_1(\omega) = \frac{1}{4\pi} \int_{-\infty}^{\infty} d\omega' \frac{\epsilon_2(\omega')}{\omega - \omega'}. \quad (33)$$

All optical response functions may now be derived from these. The optical conductivity follows:

$$\sigma(\omega) = \frac{\omega \epsilon_2(\omega)}{4\pi}.$$

If we assume the orientation of the crystal surface to be parallel to the optical axis, the reflectivity $R(\omega)$ follows directly from Fresnel's formula:

$$R(\omega) = \left| \frac{\sqrt{\epsilon(\omega)} - 1}{\sqrt{\epsilon(\omega)} + 1} \right|^2 \quad (34)$$

where $\epsilon(\omega) = \epsilon_1(\omega) + i\epsilon_2(\omega)$ is the complex dielectric function.

4. An application to $\text{Cu}_x\text{Ni}_y\text{Zn}_z$ alloys

As an initial attempt, we have applied our methodology within the framework of TB-LMTO for disordered ternary $\text{Cu}_x\text{Ni}_y\text{Zn}_z$ alloys. The alloy with the composition around 2:1:1, is known to form a solid solution of a face-centered cubic structure at the temperature 776 K [6]. Upon cooling, long range ordering takes place. All three constituent atoms in this system are in the same row of the periodic table and are neighbors. As a result we can say that there is a very small charge transfer between the constituents while forming this metallic alloy. Also the alloy should have little atomic displacement effect.

Vrijen [7] showed that the axial ratio within the fully ordered face-centered cubic phase of $\text{Cu}_{50}\text{Zn}_{25}\text{Ni}_{25}$ is unity within the experimental accuracy, confirming that lattice distortions and displacements are relatively small. The binary subsystem of this alloy consisting of Cu and Zn has already been discussed in our previous paper [8]. There we studied the effect of short ranged ordering on the optical properties of this system. We have also shown that the alloy with equal proportion of Cu and Zn is a split band and has a tendency to ordering. Using the tetrahedron approximation of the cluster variation method Rooy *et al* [9] predicted the phase diagram of a ternary $\text{Cu}_x\text{Ni}_y\text{Zn}_z$ alloy. Experimentally it has been found that the ternary $\text{Cu}_{50}\text{Zn}_{25}\text{Ni}_{25}$ alloy, in a face-centered cubic structure, exhibits a high-temperature short range order and there are two first order phase transitions occurring as the temperature is decreased. Shinya *et al* [10] have studied the short range ordering effect on this alloy by using the anomalous scattering method. They have shown that there is short ranged ordering between Cu–Zn and Ni–Zn atoms, while the correlation is in the opposite sense between Cu and Ni atoms. Because both ordering and clustering tendencies have been observed in the binary alloys of the constituent atoms, Ceder *et al* [11] supposed that the ternary alloy might exhibit interesting competing effects, and studied the stability of the face-centered cubic ground state for this alloy.

On the other hand, the experimental study of optical properties in this alloy is quite interesting. Pure Cu exhibits a main absorption edge near 600 nm and a secondary absorption structure near 300 nm. We have already discussed earlier that alloying Cu with Zn shifts the position of the main peak to lower wavelengths and the secondary peak to higher ones. For the 50–50 concentration of Cu and Zn the reflectivity curve has a sharp peak at around 540 nm, which indicates the color of the alloy. Mott and Jones [12] suggested that the main absorption edge is associated with inter-band transitions from the d-band to the Fermi-surface, and the secondary absorption edge with transition from the Fermi-surface to the higher bands. Using this suggestion the rigid-band model can interpret this behavior qualitatively. However, the shift of the absorption structures is less than the rigid-band model prediction. The model fails completely to predict the optical properties of Cu–Ni alloys with up to 25% of Ni. The positions of the main and the secondary absorption edges remain within experimental accuracy at 600 and 300 nm, respectively. This result has been explained using the concept of ‘virtual energy states’. In a Cu–Ni alloy, if Ni atoms replace Cu atoms then virtual energy states are created below and above the Fermi-surfaces. Therefore it would be interesting to study the optical properties of $\text{Cu}_x\text{Ni}_y\text{Zn}_z$ to see the effect of the extra electrons of the Zn atoms.

We have calculated the density of state for a disordered $\text{Cu}_x\text{Ni}_y\text{Zn}_z$ alloy by using the TB-LMTO-ASR method. Figure 1 shows the atom projected density of state of disordered $\text{Cu}_{50}\text{Zn}_{25}\text{Ni}_{25}$ disordered alloy in the top panel and same for the ordered alloy in the face-centered cubic structure at the bottom. We have already discussed that there is only a very small charge transfer in this alloy system. We see that the d-band of the Zn atoms is well separated from those of Ni and

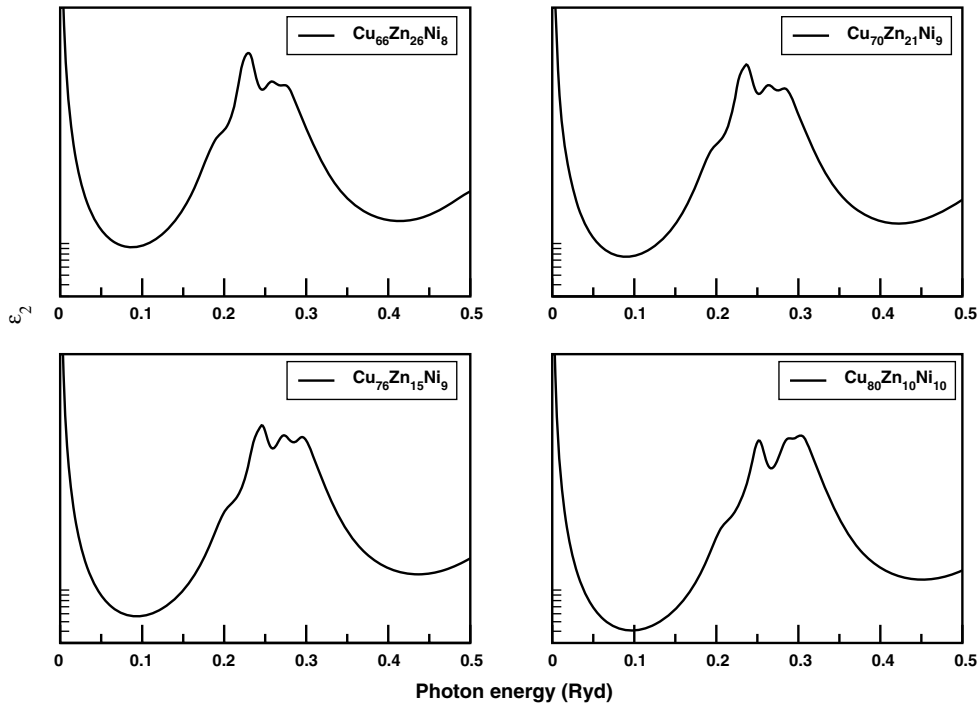


Figure 3. Imaginary part of the dielectric function (ϵ_2) of disordered $\text{Cu}_x\text{Ni}_y\text{Zn}_z$ ternary disordered alloy for four different concentrations.

Cu. Those of Ni and Cu, of course, show considerable overlap. On alloying, hybridization between Zn and Cu/Ni bands causes the single peak of Zn to break into two. There is considerable overlap between the Cu and Ni d-bands and its effect in the disordered alloy is evident, with large disordered smearing due to the scattering induced complex self-energy.

We have also applied our methodology to obtain the optical properties of ternary $\text{Cu}_x\text{Ni}_y\text{Zn}_z$ alloys. Schröder and Mamola [13] measured the absorptivity of this alloy with Ni concentration $\sim 8\text{--}10\%$ and increasing Zn concentrations from 10 to 26%. Figure 2 shows their results for percentage absorptivity as a function of wavelength in the top panel and our theoretical results at the bottom. The absorptivity for different compositions have been arbitrarily shifted vertically for better viewing.

At the lowest Zn concentration 10% experiment shows a prominent peak at 300 nm, theory yields a prominent peak at 310 nm with a weak structure at 360 nm. Presence of Zn in a Cu–Ni alloy produces a split in the absorptivity peak at 300 nm. For 15% Zn there are two structures at 310 and 350 nm, while the theory shows structures at 310 and 365 nm. With increase of Zn concentration, the new peak becomes prominent and shifts to higher wavelengths. For 21% Zn the peaks are at 320 and 390 nm while for 26% Zn they are at 330 and 410 nm. Theory shows these structures at 320 and 390 nm and 330 and 400 nm, respectively. The overall trend seen in experiments on introduction of Zn in the $\text{Cu}_x\text{Ni}_y\text{Zn}_z$ alloys where the Ni concentration is almost fixed is reproduced well in our theoretical predictions. The theory has more finer structures (particularly in the lower peak); however, given that experiments are done at finite temperatures and have their own resolutions, we do not expect to match these finer resolved structures with experiment.

It will be instructive to examine the optical conductivity. In figure 3 we present the imaginary part of the dielectric function $\epsilon_2(\omega)$ of disordered $\text{Cu}_x\text{Ni}_y\text{Zn}_z$ alloys with four different compositions: $\text{Cu}_{66}\text{Zn}_{26}\text{Ni}_8$, $\text{Cu}_{70}\text{Zn}_{21}\text{Ni}_9$, $\text{Cu}_{76}\text{Zn}_{15}\text{Ni}_9$ and $\text{Cu}_{80}\text{Zn}_{10}\text{Ni}_{10}$. The cross-over from Drude-like behavior occurs at the onset of transitions from the top of the d-bands to states above the Fermi energy. This onset energy then is an indication of the energy difference between the top of the d-band and the Fermi energy. Increasing the Zn concentration Schröder and Mamola [13] showed that the Fermi level shifts to higher energies since the number of electrons per atom increases. This is also reflected in our calculated density of state in figure 3 (top).

5. Conclusion

We have proposed a combination of the augmented space technique and the generalized recursion method of Viswanath and Müller expressed within a TB-LMTO basis (TBLMTO-AS-GR) as a suitable computational methodology for the study of optical response in ternary alloy systems. We have applied our formalism to $\text{Cu}_x\text{Ni}_y\text{Zn}_z$ alloys. Our theoretical analysis helps to understand the experimental data of these alloys from a microscopic viewpoint. We suggest the use of this technique for further studies of response functions in ternary disordered alloys.

References

- [1] Alam A and Mookerjee A 2009 *J. Phys.: Condens. Matter* **21** 195503
- [2] Viswanath V S and Müller G 1993 *The User Friendly Recursion Method* (Troisième Cycle de la Physique, en Suisse Romande)
- [3] Mookerjee A 1973 *J. Phys. C: Solid State Phys.* **6** 1340

- [4] Tarafder K and Mookerjee A 2005 *J. Phys.: Condens. Matter* **17** 6435
- [5] Hobbs D, Piparo E, Girlanda R and Monaca M 1995 *J. Phys.: Condens. Matter* **7** 2541
- [6] Rooy A D, Bronsveld P M and Hosson J 1982 *Z. Metallk.* **73** 610
- [7] Vrijen J, Bronsveld P M, ven der Veen J and Radelaar S 1976 *Z. Metallk.* **67** 473
- [8] Tarafder K, Chakrabarti A, Saha K K and Mookerjee A 2006 *Phys. Rev. B* **74** 144204
- [9] Rooy A D, van Royen E W, Bronsveld P M and de Hosson J Th M 1980 *Acta Metall.* **28** 1339
- [10] Hashimoto S, Iwasaki H, Ohshima K, Harada J, Sakata M and Terauchi H 1985 *J. Phys. Soc. Japan* **54** 3796
- [11] Ceder G, Garbulsky G D, Avis D and Fukuda K 1994 *Phys. Rev.* **49** 1
- [12] Mott N F and Jones H 1958 *The Theory of Properties of Metals and Alloys* (New York: Dover)
- [13] Schröder K and Mamola K 1968 *Phys. Rev.* **167** 658